![Sophion Bioscience logo]

Application Report

Perforated patch clamp recordings on Qube 384

Evaluation of perforating agents (nystatin, amphotericin, β-escin and gramicidin) for automated patch clamp experiments using Qube 384

Summary

In patch clamp recordings cell dialysis of intracellular constituents can be minimized by employing perforated whole-cell formation. This method allows electrical access to the cell while maintaining the integrity of the majority of cytoplasmic components. Here we report how to perform perforated patch clamp recordings on Qube 384 with or without the use of intracellular (IC) solution exchange (IC exchange).

- Recommendations for perforated patch clamp experiments with or without using IC exchange

- Comparison of four perforating agents (seal resistance, current level and success rate)

The first part of this report consists of a fast guide for using perforated patch on Qube 384, followed by an in-depth run-through of the experiments underlying our recommendations.

Introduction

In perforated patch clamp, the membrane patch in the patch hole is not ruptured as in traditional whole-cell patch clamp recordings. Instead, small amounts of pore-forming agents are introduced to the IC solution, which inserts into the membrane patch and form pores (see figure 1). This provides electrical access to the cell interior while maintaining endogenous levels of larger ions and signalling molecules[1]. Commonly used pore-forming agents are the antibiotics nystatin and amphotericin B (polyene antibiotics), gramicidin (linear polypeptide antibiotic) and β-escin (saponin derivative). For an overview of their properties see table 1.
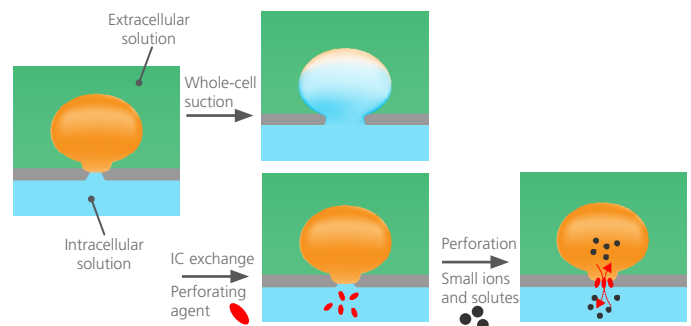
Fig. 1: Patch configurations in automated patch clamp. Standard whole-cell: From the cell-attached configuration (left) you can apply brief suction thereby rupturing the membrane to gain electrical access to the cytoplasm (top, middle). Perforated whole-cell: Perforating agent can be added using IC exchange (bottom, middle). The agent will insert into the membrane patch providing electrical access for small ions and solutes while maintaining endogenous levels of larger ions and signalling molecules (bottom, right).

Nystatin and amphotericin B: The polyene antibiotics are permeable to small monovalent cations and anions. They insert into the membrane within minutes and interfere with seal formation. Thus, they must be introduced after the seal has formed by exchanging the intracellular solution. Other challenges include that they are light and heat sensitive, losing potency over time, and cause Cl^- redistribution between the intra- and extra-cellular solutions[2].

Gramicidin D: Gramicidin D is a linear polypeptide antibiotic, which is permeable for cations but completely block the flux of Cl^- and other anions. Gramicidin perforation is slow (~30 minutes)[1] compared to nystatin and amphotericin B and it can, therefore, be introduced to the intracellular solution from the beginning of the experiment.

β-escin: The saponin-derived antibiotic β-escin forms relatively large nonselective pores that are Ca^{2+} permeable. It is hydrophilic and can, in contrast to other perforating agents, be dissolved in aqueous solutions. Also, the ionophore interferes less with seal formation and can be added directly in the intracellular solution or introduced later by IC exchange as required.

Recommendations

Experimental conditions

Our recommendations for performing perforated patch experiments on Qube 384 are summarized in Table 1 together with the general properties of the four perforating agents.

Table 1: Properties of perforating agents used in perforated patch clamp experiments and our experimental recommendations. (*) From Ishibashi *et al.*[3].

Perforant	Nystatin	Amphotericin B	Gramicidin	β-Escin
Class*	Polyene antibiotic	Polyene antibiotic	Linear polypeptide antibiotic	Saponin derivative
Pore radius*	0.4 – 0.5 nm	0.4 – 0.5 nm	≤ 0.35 nm	> 10 kDa
Selectivity*	Weakly cationic	Weakly cationic	Highly cationic	Nonselective
Conductance*	5 pS	6 pS	50 pS	?
Stock concentration	30 mM (DMSO)	30 mM (DMSO)	25 mM (DMSO)	10 mM (H_2O)
Final concentration	(100 – 200) μM	200 μM	(10 – 25) μM	(10 - 50) μM
Delivery method	IC exchange	IC exchange	Directly in IC	Directly in IC/ IC exchange

Results

To evaluate the perforating properties of four perforating agents on Qube, CHO-hERG cells were either exposed to a perforating agent or to a standard whole-cell suction protocol (see Methods section for experimental setup). The perforating agents were added using IC exchange (nystatin, amphotericin B and β-escin) or from the beginning of the experiment (gramicidin).

The average membrane resistance (R_{mem}), series resistance (R_{series}), hERG peak current (I_{max}) and cell membrane capacitance (C_{slow}) were quantified 20 minutes after IC exchange for nystatin, amphotericin B and β-escin (table 2) or in the first voltage protocol of the experiment for gramicidin (table 3). To quantify the success rate, the experiments were filtered using the following criteria

$R_{mem} > 100$ MΩ per cell

9 pF $< C_{slow} < 50$ pF

$I_{peak} > 100$ pA

In general, R_{mem} and I_{max} were slightly lower for cells in perforated as compared to standard whole-cell, likely due to the perforating agents interfering with the seal. As expected, R_{series} is elevated for cells in perforated whole-cell, due to the increased amount of membrane in the patch hole.

Table 2: List of parameters extracted for cells in perforated and standard whole-cell configuration, respectively, quantified 20 minutes after the addition of perforating agents using IC exchange. Values are average ± sem of N_{cells}.

	R_{mem} [MΩ]	R_{series} [MΩ]	I_{max} [pA]	C_{slow} [pF]	N_{cell}	Success rate [%]
Nystatin (200 μM)	954 ± 61	13.3 ± 0.5	350 ± 21	16.0 ± 0.7	75	78
Amphotericin B (200 μM)	1194 ± 97	25 ± 1	274 ± 11	15.1 ± 0.5	135	53
β-Escin (10 μM)	1152 ± 86	16 ± 1	500 ± 28	16 ± 1	54	68
Standard whole-cell	**1303 ± 48**	**11.8 ± 0.7**	**491 ± 20**	**15.1 ± 0.3**	**151**	**86**

Table 3: List of parameters extracted for cells in perforated and standard whole-cell configuration, respectively, quantified in the first voltage protocol of the experiment. Values are average ± sem of N_{cell}.

	R_{mem} [MΩ]	R_{series} [MΩ]	I_{max} [pA]	C_{slow} [pF]	N_{cell}	Success rate [%]
Gramicidin (25 μM)	201 ± 7	26 ± 1	336 ± 14	14.4 ± 0.4	139	48
Standard whole-cell	**749 ± 50**	**9.3 ± 0.4**	**517 ± 24**	**14.0 ± 0.4**	**74**	**77**

The reduced success rate of the gramicidin experiments implies that the presence of gramicidin during seal formation impacts data quality.

Spontaneous whole-cell

When performing perforated patch experiments, a small proportion (<10 %) of cells spontaneously rupture into standard whole-cell configuration. However, some transfected cell lines are fragile (depending on cell type and ion channel) and more prone to spontaneous whole-cell formation (> 50 % after 10 minutes). As part of perforated patch assay optimization, this can be evaluated by running a trial experiment, without whole-cell suction and perforating agent, to verify that the majority of the cells are in cell-attached mode during the time span of the experiment. In case of problems with spontaneous whole-cell formation, this can be remedied by lowering the holding pressure from standard (-10 mbar) to -3 mbar. For experimental protocols using IC exchange this requires a customized IC exchange block, contact your Application Scientist for more information and support.

Methods

Evaluation of patch configuration using hERG currents

Nystatin, amphotericin and β-escin were added using the Qube 384 IC exchange protocol[4]. Perforated whole-cell formation using these agents was compared to traditional whole-cell suction (figure 2). In order to evaluate the agent's ability to mediate electrical conduction, we used a CHO cell line stably expressing the human potassium channel hERG (K_V11.1). The whole-cell protocol was designed to perform two different pressure protocols in parallel within the same QChip:

Column 1-6: Standard whole-cell suction (figure 2, left)
Column 7-24: No whole-cell suction (figure 2, right)
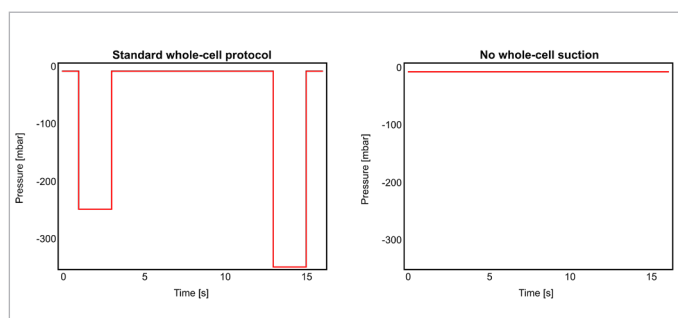
Fig. 2: Applied whole-cell protocols. Left: Standard whole-cell suction protocol applied in column 1-6. Right: No whole-cell suction applied in column 7-24.

Following the whole-cell protocol, the hERG current was recorded to evaluate electrical access to the interior of the cell (see figure 3). The cells were voltage clamped at -80 mV and hERG currents were elicited by 5 pulses comprised of a 5 s depolarization to +20 mV followed by a 5 s tail step to -50 mV (figure 3, red). Cells in a standard whole-cell configuration are expected to display standard hERG currents (figure 3, bottom), whereas the poor electrical access to cells in cell-attached mode results in very small currents (figure 3, right).
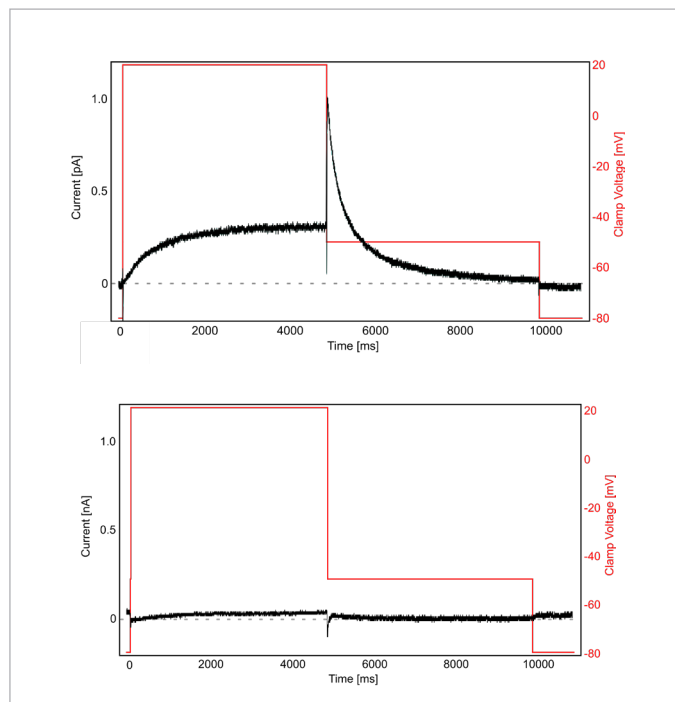
Fig. 3: Representative recordings of hERG current (black) recorded on cells in standard whole-cell (top) and cell-attached mode (bottom) in response to a voltage protocol (red) comprising a 5 s depolarization to +20 mV followed by a 5 s tail step to -50 mV.

The electrical capacitance of a cell membrane (C_{slow}) results from the lipid bilayers ability to store charges and is directly proportional to the membrane surface area ($\sim$1 µF/cm^2). A measure of the entire cell membrane can only be obtained when there is proper electrical contact to the intracellular environment. Consequently, the measured C_{slow} value is much larger for a cell in manual or perforated whole-cell configuration than for a cell in cell-attached configuration. The capacitance measure was therefore used as an indicator for whether the cell was in cell-attached ($C_{slow} < 9$ pF) or whole-cell mode ($C_{slow} > 9$ pF).

A QChip site view of single cell capacitance is displayed in figure 4, together with the corresponding hERG currents measured in the two top rows. The majority of the cells exposed to standard whole-cell suction (column 1-6) are in whole-cell mode ($C_{slow} > 9$ pF, red) whereas the majority of the cells that were not exposed to a pressure protocol (column 7-24) are in cell-attached mode ($C_{slow} < 9$ pF, blue). The configuration of the cells was reflected in the corresponding hERG currents displayed below the QChip site view.
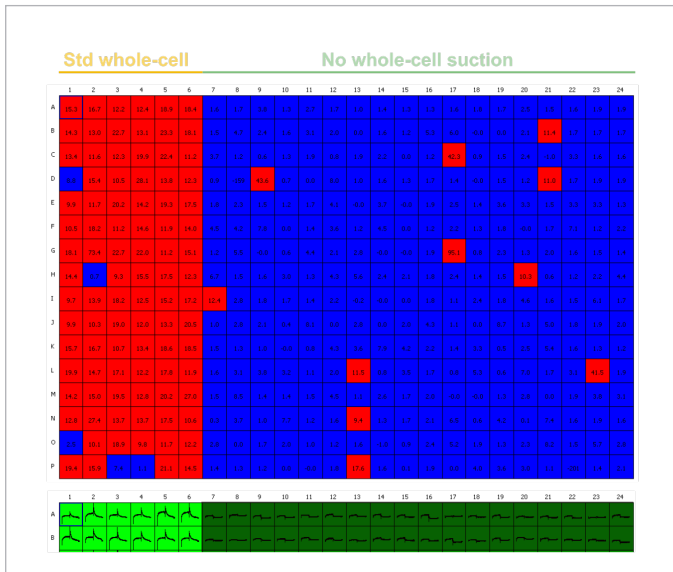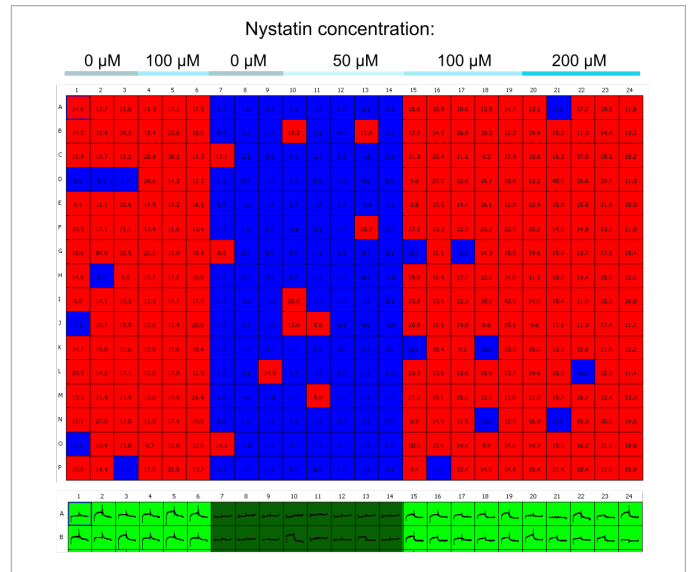
Fig. 4: QChip plate view displaying membrane capacitance (C_{slow}) measurements before exchange of the intracellular solution. Sites with $C_{slow} > 9$ pF are colour coded red and sites with $C_{slow} < 9$ pF are colour-coded blue. Column 1-6: standard whole-cell, column 7-24: cell-attached (no whole-cell suction). Below the plate view, the corresponding hERG current measurements from the top two rows are displayed (green).

Addition of perforating agent using IC exchange

Next, we evaluated three perforating agents using IC exchange. Following the initial electrical evaluation (figure 3 and 4), the intracellular solution was exchanged with solutions of increasing concentration of the perforating agent (figure 5). The IC exchange took approximately 6 minutes and was followed by two periods of 15 voltage pulses each to evaluate the electrical access.

Nystatin
First, we tested nystatin as the perforating agent. The QChip site view of single cell capacitance recorded 5 minutes after nystatin addition using IC exchange is displayed in figure 5.

Fig. 5: QChip plate view displaying membrane capacitance (C_{slow}) measurements after addition of nystatin by IC exchange. Sites with $C_{slow} > 9$ pF are colour coded red and sites with $C_{slow} < 9$ pF are colour-coded blue. Nystatin concentration: 0 µM (column 1-3 and 7-9), 50 µM (column 10-14), 100 µM (column 4-6 and 15-19) and 200 µM (column 20-24). Below the plate view, the corresponding hERG current measurements from the top two rows are displayed (green).

After addition of nystatin most of the cells exposed to 100 µM and 200 µM nystatin (column 15-19 and 20-24, respectively) entered perforated whole-cell configuration ($C_{slow} > 9$ pF, red). The configuration of the cells is reflected in the measured hERG current displayed below the QChip site view in figure 5, displaying large current peaks for cells in whole-cell and small currents for cells in the cell-attached configuration.

The rate of nystatin insertion varies from cell to cell. In figure 6 C_{slow} versus time was plotted for three single cells in cell-attached mode upon the addition of 100 µM nystatin in the intracellular solution. The figure shows how the membrane capacitance increases from ~2 pF in cell-attached mode to ~15 pF in perforated whole-cell.
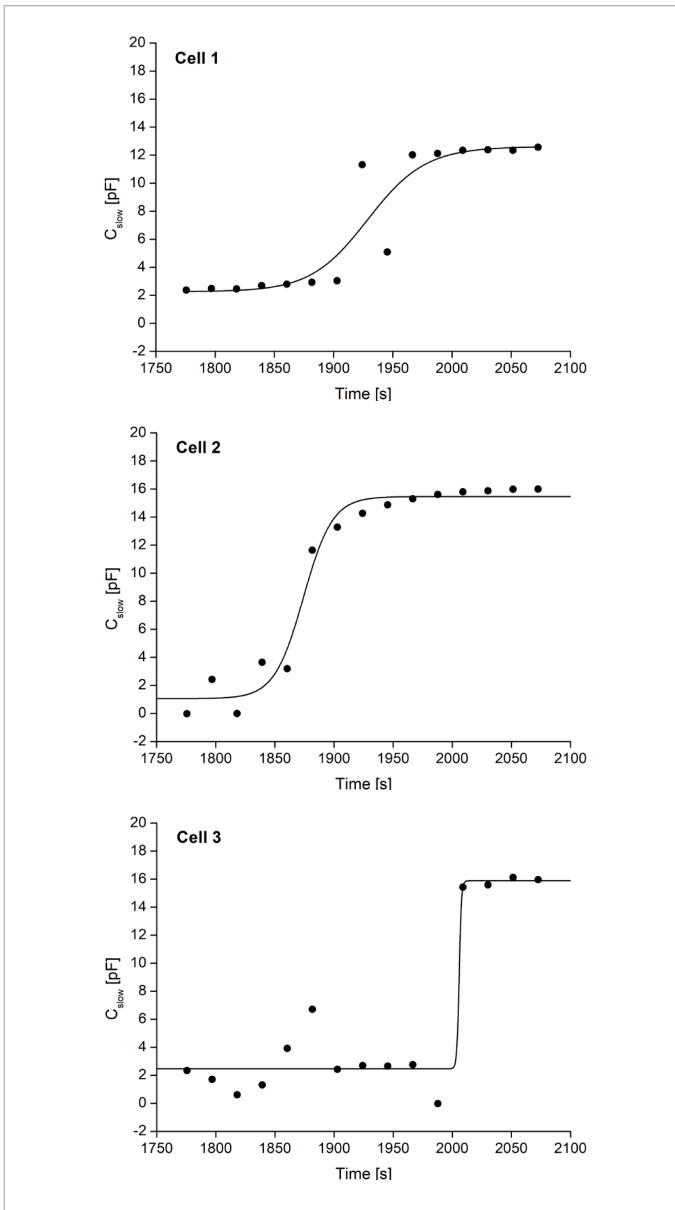
Fig. 6: The development of single cell capacitance (C_{slow}) over time upon the addition of 100 µM nystatin using IC exchange.

Fig. 7: Fraction of cells in standard or perforated whole-cell configuration (C_{slow} > 9 pF) quantified before, 5 minutes after and 20 minutes after IC exchange. The colours represent the addition of 0 µM (orange), 50 µM (light grey), 100 µM (grey) or 200 µM (black) nystatin to cells in cell-attached mode as well as cells in standard whole-cell mode (red) for comparison. Values are average ± sem between three runs and the number of cells investigated per concentration was 80 to 240.

β-Escin and amphotericin B

Next, β-escin and amphotericin B were evaluated using the same experimental procedure as described for nystatin above. The fraction of cells in standard or perforated whole-cell (C_{slow} > 9 pF) was plotted before, 5 minutes after, 20 minutes after and 30 minutes after addition of perforating agent (figure 8).

Plotting the fraction of cells in standard or perforated whole-cell configuration (C_{slow} > 9 pF) before, 5 minutes after and 20 minutes after addition of perforating agent (figure 7), illustrates that nystatin at 100 µM and above promotes perforated whole-cell formation in cell-attached cells. No effect was observed upon the addition of 50 µM nystatin as compared to the baseline (orange and grey data points in figure 7).
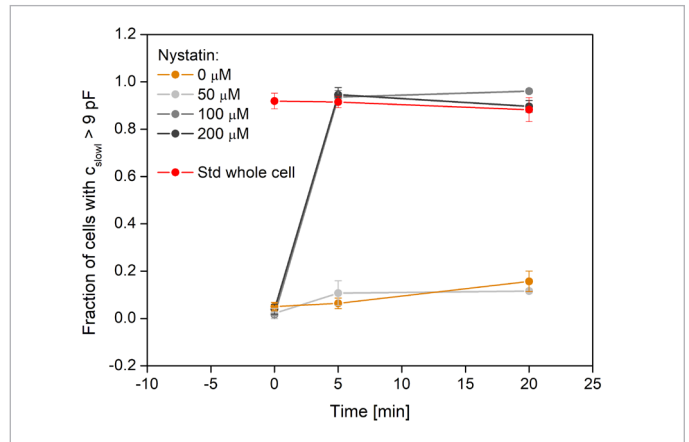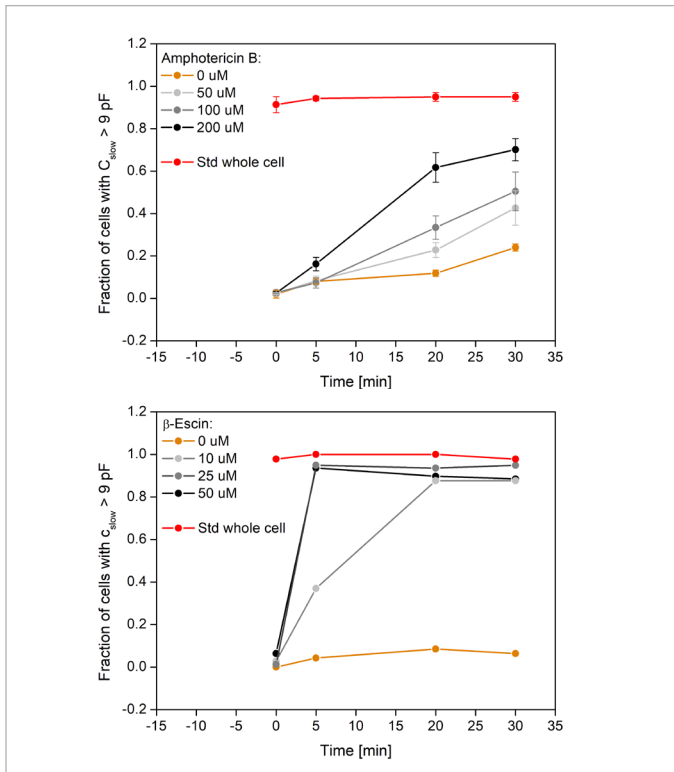
Fig. 8: Fraction of cells in standard or perforated whole-cell configuration (C_{slow} > 9 pF) quantified before, 5 minutes after, 20 minutes after and 30 minutes after IC exchange. Top: The colours represent the addition of 0 µM (orange), 50 µM (light grey), 100 µM (grey) or 200 µM (black) amphotericin B to cells in cell-attached mode as well as cells in standard whole-cell mode (red) for comparison. Values are average ± sem between three runs and the number of cells investigated per concentration were 240. Bottom: The colours represent the addition of 0 µM (orange), 10 µM (light grey), 25 µM (grey) or 50 µM (black) β-escin to cells in cell-attached mode as well as cells in standard whole-cell mode (red) for comparison. Values are extracted from one run and the number of cells investigated per concentration was 80.

Both amphotericin B and β-escin induced perforated whole-cell formation. However, although we would expect similar kinetics for amphotericin B and nystatin, perforation by amphotericin B is happening much slower (figure 8, left), possibly due to compound stickiness.

Addition of perforating agents directly in the intracellular solution

Gramicidin
The perforating agent gramicidin is relatively slow acting (30 minutes)[1] and consequently not feasible for experiments with IC exchange, in which the agent is introduced relatively late in the experiment. Instead, gramicidin was added in the intracellular solution from the beginning of the experiment.

Experiment site overviews (top six rows) of C_{slow}, R_{mem} and R_{series} values recorded in the first voltage protocol run, are displayed in figure 9. They show that gramicidin provides electrical access to the cell interior (c_{slow} > 9 pF > c_{slow}), however, as might be expected gramicidin disturbs seal formation resulting in reduced seal

resistances (R_{mem} > 200 MΩ > R_{mem}). Finally, the cells in perforated whole-cell have more intact membrane blocking the patch hole and therefore larger series resistances (R_{series} > 10 MΩ > R_{series}).
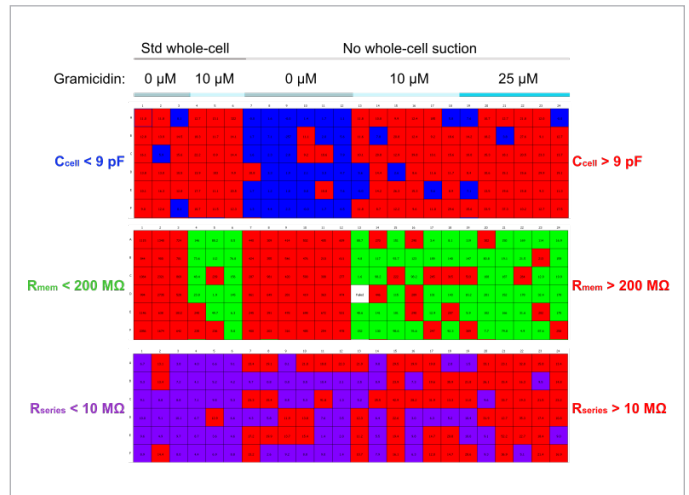
Fig. 9: QChip plate view displaying membrane capacitance (C_{slow} > 9 pF > C_{slow}) (top), membrane resistance (R_{mem} > 200 MΩ > R_{mem}) (middle) and series resistance (R_{series} > 10 MΩ > R_{series}) (bottom). Standard whole-cell suction was applied in column 1-6 and no whole-cell suction was applied in column 7-24. The intracellular solution contained 0 µM (column 1-3, 7-12), 10 µM (column 4-6, 13-18) or 25 µM (column 19-24) gramicidin.

The fraction of cells in standard or perforated whole-cell configuration (C_{slow} > 9 pF) was plotted as a function of time, with time 0 being the first run of the voltage protocol after seal formation (figure 10).
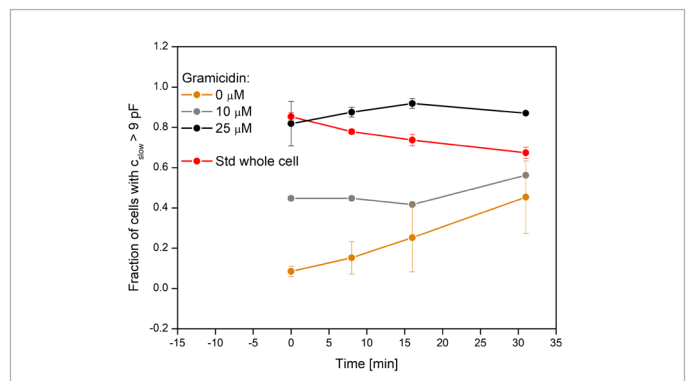
Fig. 10: Fraction of cells in standard or perforated whole-cell configuration (c_{slow} > 9 pF) quantified at 0 minutes, 8 minutes, 16 minutes and 32 minutes after experiment start. The colours represent the addition of 0 µM (orange), 10 µM (grey) or 25 µM (black) gramicidin to cells in cell-attached mode as well as cells in standard whole-cell mode (red) for comparison. Values are average ± sem between one or two runs and the total number of cells investigated per concentration were 80 to 292.

Note that compared to data recorded using IC exchange, the number of cell-attached cells spontaneously entering whole-cell mode is increased (figure 10, orange) and the number of cells in standard whole-cell (figure 10, red) is decreased. This might be due to DMSO (0.1%) being present in the intracellular solution during seal formation which is weakening the cell membrane.

Materials

Cell line:

CHO hERG DUO purchased from B'SYS.

Cell culture and harvest:

The cells were thawed according to vendors guidelines and sub-cultured according to Sophion standard operating procedures.

Cell harvest for experiments (for T175 flask):

1. Remove Culture Media and wash with 7 mL PBS
2. Add 3 ml Trypsin, gently swirl the flask and aspirate (leave about 1 mL)
3. Place the culture flask in a 37°C incubator for ~2 min (until cells have rounded)
4. Add 5 mL Serum-Free Media and resuspend the cells
5. Determine the cell density and viability and make sure that there are 2-5 million/mL cells added to the QStirrer

References:

1. Linley, J. E. Perforated Whole-Cell Patch-Clamp Recording. in Ion Channels (ed. Gamper, N.) 998, 149–157 (Humana Press, 2013).

2. Zhao, Y. et al. Patch clamp technique: Review of the current state of the art and potential contributions from nanoengineering. Proceedings of the Institution of Mechanical Engineers, Part N: Journal of Nanoengineering and Nanosystems 222, 1–11 (2008).

3. Ishibashi, H., Moorhouse, A. J. & Nabekura, J. Perforated Whole-Cell Patch-Clamp Technique: A User's Guide. in Patch Clamp Techniques (ed. Okada, Y.) 71–83 (Springer Japan, 2012). doi:10.1007/978-4-431-53993-3_4

4. Sauter, D. Internal solution exchange on Qube. 1–4 (Sophion Bioscience A/S, 2017).

Author:
Kadla R Rosholm, Application Scientist - 2019